Report of Investigations 9640

A Second-Generation Remote Optical Methanometer

Robert A. Franks, John J. Opferman, Gene F. Friel, and John C. Edwards, Ph.D.

U.S. DEPARTMENT OF HEALTH AND HUMAN SERVICES
Public Health Service
Centers for Disease Control and Prevention
National Institute for Occupational Safety and Health
Pittsburgh Research Center
Pittsburgh, PA

May 1997

International Standard Serial Number
ISSN 1066-5552

CONTENTS

ILLUSTRATIONS

TABLES

UNIT OF MEASURE ABBREVIATIONS USED IN THIS REPORT

A·Hr	ampere-hour	pct·m	percent meter
A/W	ampere per watt	pps	pulse per second
cm	centimeter	rpm	revolution per minute
cm^2	square centimeter	s	second
f	frequency in hertz	v	volt
Hz	hertz	V dc	volt, direct current
kg	kilogram	vol pct	volume percent
m	meter	W	watt
min	minute	µm	micrometer
mm	millimeter	°C	degree Celsius
pct	percent		

OTHER ABBREVIATIONS AND ACRONYMS USED IN THIS REPORT

AGC	automatic gain control	op amp	operational amplifier
C	concentration	Quad	quadruple
CH_4	methane	RC	resistive-capacitive
CMOS	complementary metal-oxide semiconductor	ROM	remote optical methanometer
		SPST	single-poll single-throw
dc	direct current	α	absorption coefficient
DIP	Dual In-Line Pack	π	constant pi (3.14159)
FET	field effect transistor	τ	time constant
IC	integrated circuit	υ_3	Spectroscopic name for the fundamental absorption band caused by the vibrational-rotational transition of the methane molecule
IR	infrared		
LCD	liquid crystal display		
N_2	molecular nitrogen	ℓ	length
NEP	noise effective power		

Mention of any company name or product does not constitute endorsement by the National Institute for Occupational Safety and Health.

To receive additional information about mining issues or other occupational safety and health problems, call 1-800-35-NIOSH (1-800-356-4674), or visit the NIOSH Home Page on the World Wide Web at http://www.cdc.gov/niosh/homepage.html

A SECOND-GENERATION REMOTE OPTICAL METHANOMETER

By Robert A. Franks,[1] John J. Opferman,[2] Gene F. Friel,[3] and John C. Edwards, Ph.D.[4]

ABSTRACT

As the use of deep-cut mining increases, there is expected to be a greater demand for methane (CH_4) measurement devices capable of scanning working faces at depths in excess of 10 m to alert mine personnel of hazardous concentrations of CH_4 and to satisfy regulatory requirements. Remote optical devices offer the most promise to satisfy these objectives while the operator remains safely under supported roof. A second-generation remote optical methanometer (ROM) has been designed and is undergoing laboratory evaluation at the National Institute for Occupational Safety and Health.[5] It operates on the principle of differential absorption of the "υ_3" fundamental absorption band of CH_4 centered at 3.31 μm in the infrared region of the spectrum. The new instrument differs from the previous prototypes by the replacement of the two-band pass differential absorption technique of measurement with a single- filter gas correlation technique and a refinement of the amplifier and gating circuitry used within the unit. This results in a more accurate isolation of the CH_4 spectral absorption band centered at 3.31 μm. A specially designed 0.4-m-diam variable-length gas mixing tunnel was constructed and instrumented with CH_4-sampling capability to calibrate the ROM. Experiments have demonstrated the ability of the detector to respond to various conditions of CH_4 (pct•m) at distances as great as 12 m. Thermal radiation generated within the instrument is the controlling factor in the drift of the output signal and, therefore, the reliability of the instrument. Several approaches to reduce this extraneous radiation interfering with the infrared detector are described, such as the installation of a fan in the instrument and thermoelectric coolers on the detector's heat sink. Implementation of this technology will significantly improve the safety of miners.

[1]Electronic engineer.
[2]Electronics technician.
[3]Chemical engineer.
[4]Research physicist.
Pittsburgh Research Center, National Institute for Occupational Safety and Health, Pittsburgh, PA.
[5]This research originated under the former U.S. Bureau of Mines prior to transferring to the National Institute for Occupational Safety and Health in 1996.

INTRODUCTION

Methane gas (CH_4) is a mining hazard that requires constant measurement and control. A natural byproduct of coal that is released during mining, CH_4 is explosive when mixed with air at concentrations from 5 to 15 vol pct; it is most explosive when occurring at the stoichiometric concentration, 9.8 pct. CH_4-air explosions can initiate more devastating coal dust explosions as the thermal ignition and aerodynamic source. Cognizant of this, Federal regulations [30 CFR[6] 75.362 (1996)] require on-shift examination at 20-min intervals, or more frequently, during operation of equipment in the workplace. As an added precaution against mine explosions, CH_4 monitors are required to be installed on mining machines used to extract or load coal, and the monitor must give a warning at 1 pct CH_4 and deenergize the machine on which it is mounted when the CH_4 concentration reaches 2 pct [30 CFR 75.342 (1996)]. Because the molecular weight of CH_4 is only slightly greater than one-half that of air, it can form a roof layer in a mine and, through transport by the entry airflow, quickly extend its zone of influence to mine sections that are relatively free of CH_4 sources. It may, in this mode, act as a path for ignition propagation to a region containing coal dust that is not properly protected by rock dusting.

Two measures exist to deal with CH_4 in a mine. One is to deplete the coal seam of as much CH_4 as possible through CH_4 drainage techniques. However, this method is not in itself adequate to control CH_4 in a mine. This method is dependent upon the coal having an adequately high permeability for differential pressure methods to overcome the coal's aerodynamic resistance to CH_4 outgassing. CH_4 drainage applications represent a major prevention effort. However, the efficiency of this technique is never adequate to guarantee that CH_4 concentrations will be below the explosive limit.

A second measure is to dilute the CH_4-air concentrations and simultaneously remove the CH_4 from the mine airways using adequate ventilation airflow. This approach can be improved through the application of a predictive ventilation computer program [Edwards and Li 1984] to the mine network. This program determines the expected CH_4 concentration based on changes in ventilation with known measured CH_4 concentrations for a specified ventilation plan. Even though sufficient ventilating air may be present to reduce the average CH_4 to concentrations well below the explosive level, CH_4 could still accumulate within certain areas, such as dead-ended face areas. If the latter should occur, line brattices or other ventilation devices would be required.

[6] *Code of Federal Regulations*. See CFR in references.

A significant factor in both of these measures for the control of CH_4 is detection through frequent, and often continuous, monitoring of mine air. The earliest CH_4 detector was the flame safety lamp. The flame safety lamp was a gas (carbide) lamp with a flame calibration scale on the shield and was used by a fire boss while making preshift inspections. The lamp used calcium carbide immersed in water to produce acetylene gas that was used for fuel for the flame. An increase in the flame size indicated the presence of a combustible gas; a reduction indicated oxygen depletion (blackdamp). The flame safety lamp was reliable and durable, but was only an indicator of CH_4 and not a quantitative measurement of CH_4 concentration. Modern CH_4 sensors are based on thermal, electrochemical, or optical technologies [McPherson 1992]. The standard usage of each method is for a point measurement of CH_4. With the increase in deep-cut mining, it is expected that there will be a greater need for safely monitoring face areas in excess of 10 m as they are being developed. One obvious candidate for safe, mobile detection is a remote optical instrument that analyzes the reflected light from coal mine surfaces while the operator remains under permanently supported roof.

Westinghouse Electric Corp. developed under contract with the former U.S. Bureau of Mines a remote optical methanometer (ROM), which was previously evaluated [Franks et al. 1986]. This first-generation ROM measured the differential absorption of CH_4 with two band-pass filters, one centered at 3.31 μm (an absorption band for CH_4) and the other centered at 3.45 μm (slightly outside the CH_4 absorption band). The instrument responded inadequately to CH_4 in controlled experiments. Based on these results, a second-generation ROM was developed by Westinghouse that incorporated two major changes: (1) the use of a continuous light source instead of a pulsed flashlamp and (2) the use of a single infrared detector instead of two detectors. Both improved design features were incorporated into this new prototype. Recently, a major change was incorporated into the instrument that enables the detector to evaluate the reflected light at the isolated 3.31-μm line. This involves the replacement of the two band-pass filters with a single band-pass filter and two gas correlation cells. This technique provides a more accurate determination of the light attenuation due to CH_4 absorption along the optical path between the detector and the reflective coal surface. The two gas correlation cells also make the measurement specific to CH_4.

This report describes the theory of operation of this second-generation ROM and initial testing of the new prototype.

PRINCIPLE OF OPERATION

The ROM is an open-path optical CH_4 detector that uses light reflected from mine surfaces to measure the CH_4 concentration over the path length. The target range required of an ROM at this time is 10 m. Figure 1 shows the second-generation ROM, which has dimensions of 18 cm by 43 cm by 54 cm and weighs less than 17 kg. The unit has three principal components: (1) a light source, (2) a collecting system with an electronic signal-processing unit, and (3) a battery module. Each component is described in detail below.

GENERAL THEORY

The ROM's operation is based on infrared light absorption. As light passes through the atmosphere, certain frequencies of the light are absorbed by the gases in the atmosphere. These missing frequencies are specific for a given gas and correlate to particular rotational and vibrational states of the absorbing gas. These missing frequencies are called spectral absorption lines. A gas detection method that is based on this phenomenon is called differential absorption.

All of the prototype ROM's sponsored by the National Institute for Occupational Safety and Health (NIOSH) prior to the current one have been based on differential gas absorption. In this technique, infrared radiation is measured at two different frequency bands—one band coincident with a specific gas absorption line, the other very close but not coincident with the absorption line. When the measured gas is introduced into the optical path of the instrument between the light source and the detection optics, the measured band coincident with the absorption line will have reduced amounts of radiation pass from the source to the detector, while the other band, not coincident with the absorption line, will be unaffected. Therefore, a calculation of the ratio of the measured signal from the absorption band to the measured signal from the nonabsorption band will be inversely proportional to the concentration of the gas in the optical path measured in pct•m.

The current model is based on a revision to this technique called gas correlation. In this technique, the infrared radiation is measured in only one band, but it is measured in two different ways. The first way in which it is measured is after the radiation has passed through a sample of the gas under test at a specific concentration. The second way is after the radiation has passed through an inert sample of gas contained in the same manner as the gas under test. The radiation signal passing through the gas under test will have much of the light in the band of interest removed by passing through the test sample. This significantly blocks the capability for further light absorption for the associated measurement. When the measured gas is introduced into the optical path between the light source and the detector, the measurement made via the inert sample will be reduced more significantly than that made via the gas-under-test sample because of the reduction in the absorption capability for the latter measurement. Therefore, the calculation of the ratio of the measured signals from both measurement conditions will again be inversely proportional to the concentration of gas in the optical path measured in percent meters.

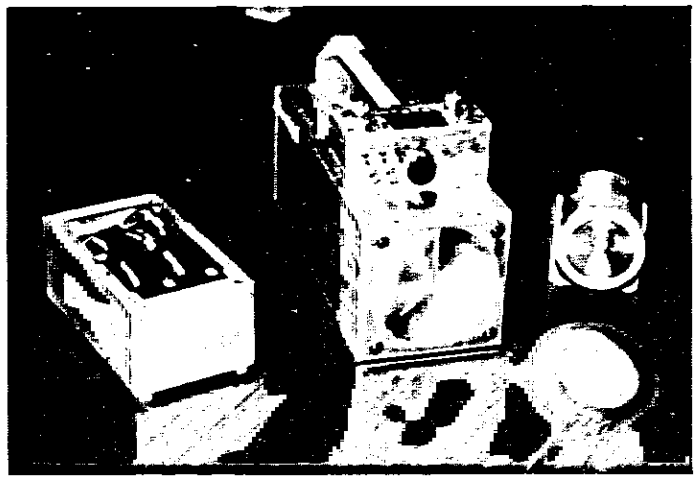

Figure 1.—Second-generation remote optical methanometer (ROM).

The gas correlation method has two major advantages over the differential absorption method of gas detection. First, it is very specific to the particular gas under test. There is no cross measurement from other gases of similar characteristics. It was noted that ethane, a minute component of natural gas, created a significant interference with CH_4 measurements when testing previous prototypes. Second, the gas correlation method isolates a particular radiation band of interest in which all of the measurements are made. This compensates for any changes in reflectivity or radiation transmission strength that may occur between different radiation bands.

OPTICAL

The ROM is equipped with a 90-W axial filament quartz-halogen incandescent lamp as the light source. The lamp is mounted in its own housing, which is attached to the front top of the unit. The lamp housing contains a highly reflective parabolic mirror (manufactured by Melles Griot) to concentrate the light into a parallel beam with a divergence of less than 0.50 m per 10.67 m of path length. A sapphire window is used on the front of the lamp housing to protect the bulb and prevent spectral loss through the window. The source beam is projected forward from the instrument toward a mine surface within an entry under test.

The reflected light from the mine surface is collected by a Fresnel lens with both a focal length and diameter of lens of 15 cm that focuses the light onto the detector. The reflected light passes through two absorption cells that are mounted on a filter wheel attached to the detector housing 3 to 5 cm in front of the detector. The filter wheel, rotating at 4,400 rpm, is driven by a 12 V dc micromotor and alternately passes the reflected

light through these two 2.54-cm-diam by 1-cm-long absorption cells onto the detector (a secondary double convex lens is located behind the filter wheel to augment the collection of reflected light). One cell is filled with pure nitrogen (N_2), the other with pure CH_4. Between the filter wheel and the detector is also mounted a dielectric optical notch filter centered at approximately 3.31 μm, the center of the principal CH_4 absorption line, and with a transmission width equal to that of the absorption line. These two small metal cylinders with quartz windows (absorption cells), in conjunction with the optical notch filter, are the basis of the gas correlation technique described previously. The detector used is an EG&G Judson J12 series indium arsenide 2-mm-diam infrared detector.

This particular Judson J12 detector is cooled with an internal two-stage thermoelectric cooler to maintain the surface temperature of the detector between −40 °C and −60 °C. The precise temperature depends on how well the heat is removed from the detector enclosure base. The detector has a natural spectral bandwidth from 1.0 to 3.8 μm, a responsivity of 1.5 A/W peaking at 3.3 to 3.5 μm, and a D* detectivity[7] of 10^{10} cm•$Hz^{1/2}$•W^{-1}. The detector acts as a photodiode.

SIGNAL PROCESSING

A block diagram of the ROM is shown in figure 2. The electronics has boards grouped into six functional units. These electronics boards are: (1) power, (2) thermoelectric cooler, (3) data display and alarm, (4) gating and timing, (5) analog processing, and (6) main amplifier.

The detected signal first enters the instrument's electronic subsystem for processing and analysis as an output current from the Judson J12 detector. The output current from the detector is then collected by a PA-5 transimpedance (current-mode) preamplifier (also built by EG&G Judson) with a transimpedance gain of 10^6 and converted into a voltage signal.

Main Amplifier

The output signal from the PA-5 preamplifier is fed through the main amplifier board. This board provides a maximum voltage gain of $2.5\times10^{+3}$ and amplifies the instrument's retrieved signal to the 10-V range used for processing. The main amplifier board contains a four-stage operational amplifier circuit with low-pass filtering, offset adjustment, and variable gain. The low-pass filter reduces wide band random noise. The circuit uses a Burr Brown OPA-121 op amp in the inverting mode for each stage. Filtering is provided by capacitance in the feedback circuit of the first stage of the amplifier. The main amplifier board has a direct-current (dc) clamping circuit at the input to provide zero reference for the subsequent amplification process and an optical coupler circuit at the output to provide maximum isolation between this noise-sensitive, high-gain amplifier and the subsequent processing circuitry.

Main Analog Processor

At the output of the main amplifier, the signal is composed of a train of 10-V pulses at a frequency of 147 pps that are generated from the filter wheel, spinning at 4,400 rpm, rapidly placing each of the two absorption cells in front of the detector (a chopping effect). This train of pulses is then divided into separate components, one pulse train for each of these two cells, made up of the pulses associated with that cell. A signal is then generated for each pulse train that is proportional to the running amplitude average of that pulse train for a certain sliding time window (time constant). This is accomplished by the main processor board. The circuit elements that separate out the pulses from the N_2-filled absorption cell are designated the signal channel; the circuit elements that separate out the pulses from the CH_4 filled absorption cell are designated the reference channel. Each produces an integrated dc output signal that was measured during calibration experiments that were conducted in a tunnel described later in this report.

The main processor board is a combination of four separate circuit sections: an automatic gain control (AGC) circuit, an analog solid-state switch bank, a balancing amplifier bank, and an integrator bank. The three latter sections are called banks because they are made up of two components each, one for each channel.

The AGC circuit is composed of a Burr Brown DIV 100 divider module that acts to amplify or attenuate the incoming signal to maintain a constant signal level at the integrators despite fluctuations in reflected light due to hand motion with the instrument. This is accomplished by monitoring the amplitude of the pulse train from the reference channel at the input to its integrator stage and then generating an AGC signal of proper polarity and amplitude to compensate for any signal fluctuations. To produce the AGC signal, the pulse train is converted into a peak-detected dc signal, scaled, filtered to reduce ripple, and inverted to the proper polarity. This signal is then used as the driver signal for the DIV 100 denominator input. The incoming signal channel from the main amplifier board is fed into the numerator input. The AGC is switch-selectable between constant OFF, constant ON, and AUTOMATIC. In the constant OFF mode, the denominator input is set at a fixed dc level generated by a voltage divider. In the constant ON mode, the denominator is locked to the AGC feedback circuit described

[7]D-Star (D*) detectivity is a relative sensitivity parameter used to compare performance of different detector types. D* is the signal-to-noise ratio at a particular electrical frequency and in a 1-Hz bandwidth when 1 W of radiant power is incident on a 1-cm^2 active area detector. The higher the D* value, the better the detector:

$$D^*_{(cm\times Hz^{1/2}\times W^{-1})} = \frac{[\text{ActiveArea}_{(cm^2)}]^{1/2}}{\text{NEP}_{(W/Hz^{1/2})}}.$$

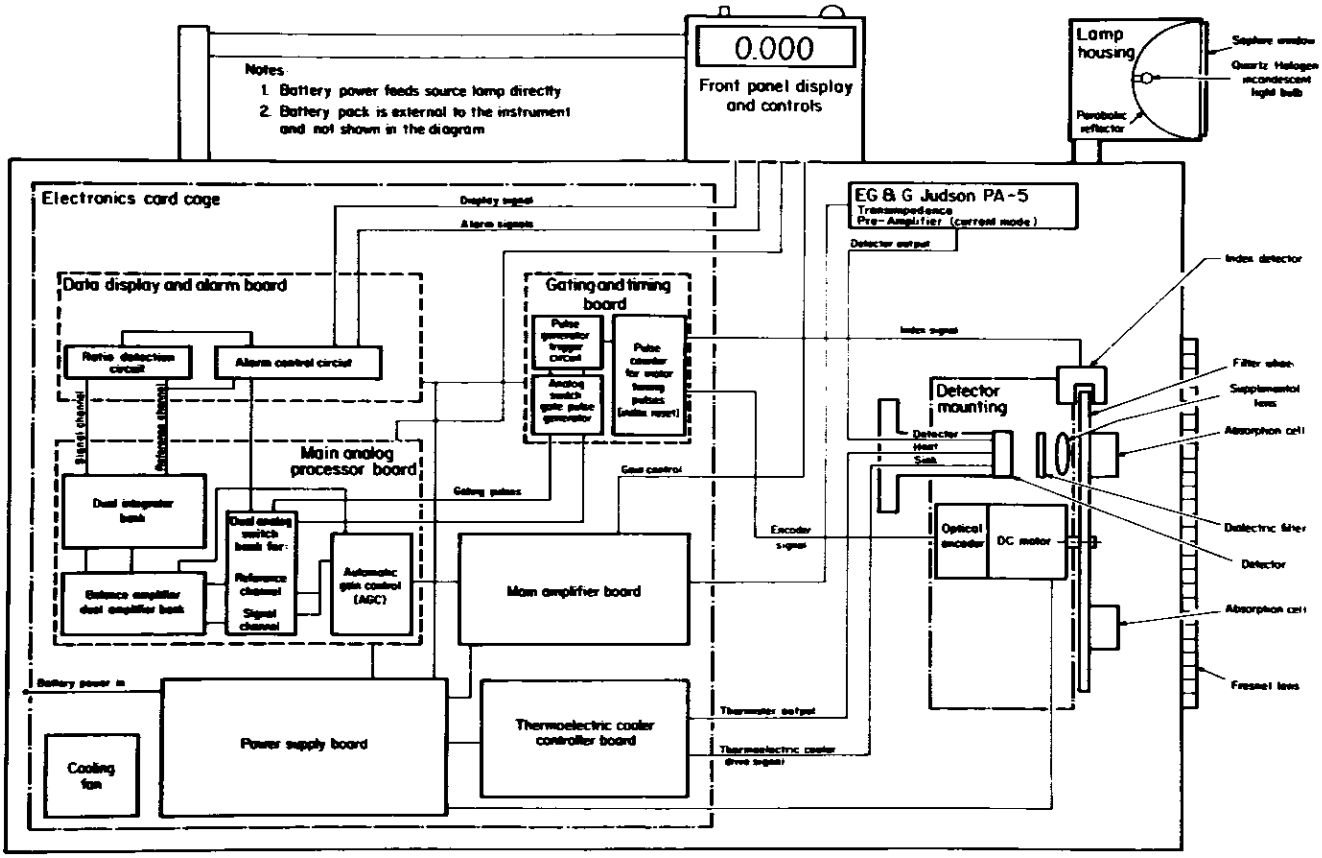

Figure 2.—Block diagram of remote optical methanometer (ROM).

above. In the AUTOMATIC mode, the AGC switches to a fixed denominator level from the AGC feedback circuit when the integrator level goes outside a predetermined signal OK level (front panel indicator). It should be noted that the AGC has a fixed dynamic range that cannot compensate for gross loss of signal.

The output of the AGC is fed through another dc clamping circuit to ensure that zero reference is maintained and into the analog switch bank. The analog switch is constructed of a DG201 Quad CMOS single-poll-single-throw (SPST) analog switch module (a solid-state relay module). Two of the four relay switches are used. The signal from the dc clamping circuit at the output of the AGC is routed to the throw arm input (usually the source input to an FET) of the two relays used. The contact side of the switch serves as the output, creating the two channels of the instrument as described above, the reference channel and the signal channel. The relay actuator input to the two switches (the FET gate input) is fed by signals from the gating and timing board, which is described later. The gating and timing board takes triggers from the filter wheel and the filter wheel motor and generates the gating pulses for the analog switch bank at the correct time and duration to permit the complete absorption cell signal pulse to pass into the relevant channel integrator.

The two individual signals pass to the balance amplifier bank. The reference channel signal passes through a unity gain inverting amplifier, while the signal channel signal passes through a variable gain inverting amplifier with a maximum gain of two. This amplifier's gain is controlled with a front panel balance knob. This permits the instrument to be balanced for a zero CH_4 reading in a clean atmosphere.

Both signals from the two channels now pass into the integrator bank. This stage is made up of two identical integrators, one for each channel. The integrators are composed of practical op amp integrator circuits that use a parallel RC feedback circuit to eliminate offset voltage buildup on the integrator. The cutover frequency of the practical integrator circuit, $f_c = 1/(2\pi R_f C_f)$, is used to limit the integration period. The integrator circuit will not function as an integrator for frequencies less than this cutover frequency or, inversely, for time periods greater than the time constant, $\tau_c = R_f C_f$ of the feedback circuit. The integration period is controlled by a front panel control and sets $\tau_c = 0.3$, 1.0, or 3.0 s. The output of each of these two integrators is a dc signal that is the accumulation of the gated detector returns (only as the respective absorption cell passes the detector) for the respective channel for a period of τ_c. These two signals are the main outputs for the main analog processor board and are two of the four signals acquired during the calibration experiments.

Data Display and Alarm

Signal flow now moves to the display and alarm board. This circuit board is the heart of the instrument. It takes the accumulated channel signals and uses them to determine if an excess of CH_4 is apparent in the optical path or not. To do this, the incoming signals are fed into an Analog Devices AD534 Internally Trimmed Precision IC Multiplier configured to act as a divider circuit. The signal channel (V_S) is fed into the numerator input, and the reference channel (V_R) is fed into the denominator input of the AD534. The output equation for this divider is

$$V_O = 10\left(\frac{V_S}{V_R} - 1\right). \quad (1)$$

This output signal is now inverted before being used to provide a final signal formula of

$$V_O = 10\left(1 - \frac{V_S}{V_R}\right). \quad (2)$$

As can be seen from the instrument's output equation, the unit will read zero volts when properly balanced, $V_S = V_R$, in clear air. As CH_4 enters the optical path, V_S will tend to be reduced to a greater extent than V_R, thereby causing the output voltage, V_O, to rise to increasing positive values.

This board also generates the instrument's front panel alarms, which also control the AGC circuit in AUTOMATIC mode. The reference signal from the reference channel integrator is measured by a comparator circuit for a high or low out-of-range signal. This signal is displayed as the instrument's SIGNAL OK indicator and in AUTOMATIC mode also controls the AGC circuit. When the SIGNAL OK indicator is off, the AGC is in constant gain mode; when the SIGNAL OK indicator again returns to on, the AGC is returned to variable gain mode after an appropriate delay to allow the instrument's integrators to stabilize. This prevents the AGC from going into dc saturation for very low reference channel signal values. The SIGNAL OK indicator also controls another DG201 analog switch that feeds the resultant V_O output signal from the data display and alarm board to the display. When this indicator signal is ON, the output signal is fed to the display and when it is OFF the output signal is blocked.

The instrument's output signal, V_O, is finally sent to the Modutec BL176301 digital panel meter on the front panel for display. The display is a 3-1/2 digit LCD display setup to read from −20.00 V dc to +20.00 V dc. The maximum range of the output signal, V_O, is +15.00 V dc to −15.00 V dc. The instrument is maintained at slightly less than 0.0 V when balanced in clear air and would reach values of +0.50 to +1.0 V during tests in the calibration tunnel.

Auxiliary Circuit Boards

Three auxiliary circuit boards are necessary to complete the circuitry used to operate this instrument. The first is the gating and timing board. This board has as its input two sets of pulses associated with the filter wheel. The first pulse input comes from an index notch detector mounted directly on the filter wheel/detector mounting assembly. The filter wheel has a small index notch cut in the aluminum rim of the wheel. The wheel itself is a solid aluminum disk, except for the two window orifices with their respective absorption cells mounted over them and the small notch in the rim of the wheel. Mounted down over the rim is a TRW Optron OPB848 Slotted Optical Switch that makes optical contact each time the wheel rotates the notch past this switch. This results in transmitting a reset pulse through the gating and timing board. The second pulse input comes from the optical encoder mounted on the back of the MicroMo 1624T012S02A 12 V dc micromotor. The encoder generates 15 quasi-sinusoidal pulses for each revolution of the motor shaft coincident with particular shaft azimuth locations. These pulses are fed to the gating and timing board as clock pulses. The gating and timing board has a Texas Instruments SN74HC193N Binary Synchronous 4 Bit Up/Down Counter that is reset by the index pulse and then counts the encoder pulses generating four-bit binary words indicating filter wheel position. The gating and timing board also has a bank of two TI SN74HC85N 4 Bit Magnitude Comparitors, one for each channel, that compares this position word to a DIP switch-selectable preset word. When the two words match for a particular channel, the respective four-bit magnitude comparator triggers the associated adjustable-width Harris CD74HC221E One Shot Multi vibrator, also in a bank of two. The One Shot Multi vibrator signal is used to open that channel's DG201 analog switch on the main analog processor board for its proper duration to pass the associated signal pulse. This constitutes the two output signals for the gating and timing board mentioned earlier.

The next essential auxiliary circuit board is the thermoelectric cooler controller board. This circuit maintains the −40 °C to −60 °C detector temperature by driving the detector's internal two-stage thermoelectric cooler. The board derives its input signal from an internally mounted thermistor within the detector case. This thermistor is connected as a component in a voltage divider spanning between common and +5 V dc power. This divider generates a signal that is inversely proportional to the temperature of the detector; the lower the temperature, the higher the signal. This is algebraically differenced against a preset adjustable set point. When the detector is at the set temperature, the difference signal is zero. This difference signal is then integrated, inverted, and fed to the cooler driver circuit as the activation signal for the cooler. When the instrument initially comes on, the detector temperature is high and the thermistor signal is low. The integrator accumulates a large positive signal driving the cooler, which sends the detector temperature

downward toward the set point. When the set point is reached, the thermistor signal rises and balances the negative set point. The integrator accumulation drops to zero, and the cooler current drops back to a low maintenance value. The detector temperature will float up and down around the set point as heat is gained by the detector enclosure from the surrounding environment and the controller intermittently produces more drive signal to the cooler to compensate. It should be noted that auxiliary thermoelectric cooling experiments are underway to provide active cooling to the heat sink assembly in which the detector enclosure is mounted, as this area is experiencing a heat buildup that is interfering with the detector operation after prolonged use of the instrument.

The final essential auxiliary circuit is the power supply board and associated battery assembly. The instrument power is derived from two 6-V Eagle-Picher CFM6V10 10-A•Hr batteries comprising the unit's 12-V battery bank. This 12-V supply is used to directly operate the 100-W quartz halogen lamp source, power the 12-V micromotor after passing through a noise filter to eliminate feedback motor noise, and as input to the power supply board. Each battery is also switch-selectable to drive the detector's two-stage thermoelectric cooler driver circuit. On the power supply board, the 12-V power is connected as the source power for an Analog Devices AD-953 DC to DC Converter. The output of this module is +15 V, −15 V, and common to power the instrument's electronics. This power is again filtered at the power supply board prior to its use for the electronics. There are also taps taken for regulated +12 V, −12 V, and +5 V by using National Semiconductor LM78L12AC, LM79L12AC, and LM78L05AC regulators off of the two 15-V leads. The two regulated 12-V taps are used to power the Judson PA-5 preamp. The regulated +5-V tap is used to operate the logic circuits on the display and alarm board.

CALIBRATION

CALIBRATION TUNNEL

The ROM does not measure a specific pct CH_4 at a point, but rather the integrated average of the CH_4 concentration over the path length. This value can be related to conditions that favor a CH_4-air ignition that can result in a transition to a coal dust explosion. There is a minimum volume of CH_4 required for this event.

This idea of CH_4 pct•m over an optical path led to the development of a calibration method for evaluating the instrument's reference and signal channel ratio for a specific CH_4 pct•m using at least two different path lengths and CH_4 concentrations. To accomplish this, a calibration tunnel was constructed. With the use of 3-m-long segments of 0.4-m-diam mine ventilation tubing, the length of the tunnel could be varied by adding or removing segments of the tubing. At one end of the tunnel, there was a gas mixing fan and at the opposite a target painted with black paint to simulate a coal surface. The light from the ROM, located near the fan, was directed at the target. Leakage of the calibration gas mixture at the segment joints was prevented by wrapping household-grade plastic wrap around the tubing. A controlled volume of 4.5 pct CH_4 in nitrogen was passed from a cylinder through a plastic tube into the tunnel. Nitrogen was used for safety considerations. After the appropriate volume of CH_4 measured by a gas volume meter was fed into the tunnel, a solenoid check valve, which was open during the CH_4 introduction to maintain one atmosphere pressure, was closed. At this point, the mixing fan was started. To promote rapid mixing, a flexible 15-cm-diam bypass tube was connected to the tunnel behind the fan and at the opposite end near the target. Sample tubing was connected to each end of the tunnel and, through a sequence of valves, gas from the tunnel was fed through an infrared CH_4 analyzer. When the same CH_4 concentration was measured at each end of the tunnel, mixing was considered to be complete and the blower fan was shut off. The ROM lamp was turned on, and the ROM reference, signal, and ratio data, as well as the infrared CH_4 analyzer data, were acquired with an analog-to-digital data acquisition system. After sufficient data were acquired, the above procedure for adding CH_4 to the tunnel was repeated and the measurements made for a new CH_4 pct•m value. When sufficient data had been acquired for a fixed tunnel length, which generally was three CH_4 concentration values, the tunnel was purged of CH_4 and another 3-m segment was added to the tunnel. The entire calibration process was then repeated. The maximum CH_4 concentration in the tunnel never reached 1 pct of actual gas concentration as measured by the pump-driven infrared CH_4 analyzer. The pct•m value, which is a calculated product of concentration and path length and is the instrument's measured value, will be large for small pct CH_4 concentrations over long path lengths. Figure 3 shows adjustments being made to the ROM prior to an experiment.

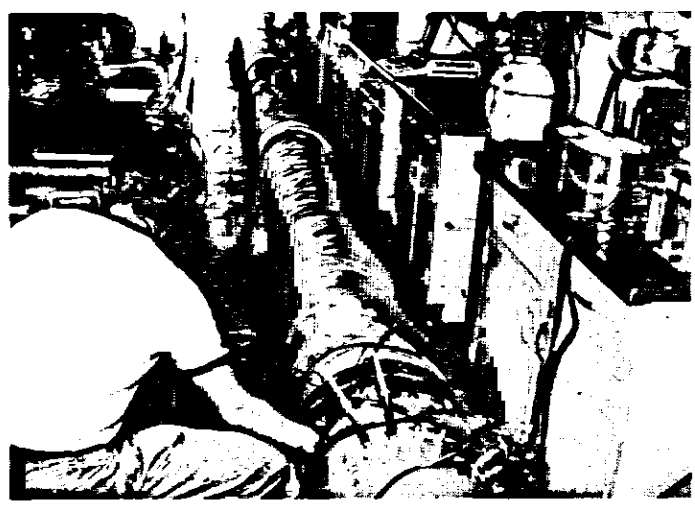

Figure 3.—Adjustments being made to ROM in calibration tunnel.

CALIBRATION RESULTS

A series of 12 experiments (A through L) was conducted in the calibration tunnel. Each experiment used on the average four different CH_4 concentrations. Table 1 lists the detector-to-reflector length for each experiment, as well as the maximum CH_4 pct•m for the experiment.

Table 1.—Experimental conditions

Experiment	Tunnel length, m	Maximum CH_4 pct•m
A	3.0	0.79
B	3.0	0.80
C	5.7	1.42
D	6.1	1.21
E	6.1	1.41
F	6.1	1.41
G	6.1	2.37
H	8.5	1.98
I	8.5	2.23
J	8.5	2.32
K	11.6	2.87
L	11.6	4.03

The measurable quantity of interest is the ratio as expressed by equation 2. However, to account for different initial values of the integrated signal and reference channel voltages, V_S and V_R, their values are normalized by the ROM lamp-on and lamp-off condition. The new definition of RATIO is given by

$$\text{RATIO} = 10\left(1 - \left(\frac{\hat{V}_S}{\hat{V}_R}\right)\right), \qquad (3)$$

where

$$\hat{V}_S = \left(\frac{(V_S - V_S^{OFF})}{(V_S^{ON} - V_S^{OFF})}\right),$$

and

$$\hat{V}_R = \left(\frac{(V_R - V_R^{OFF})}{(V_R^{ON} - V_R^{OFF})}\right).$$

An explicit application of equation 3 is shown in figure 4 for experiment F as the calculated ROM ratio. All measured data were mathematically smoothed to eliminate detector noise. The sharp peaks in CH_4 as measured by the infrared analyzer during injection of the bottled gas correspond to sampling at the end of the tunnel where CH_4 is injected. Following the CH_4 injection, the flat profile of the CH_4 concentration corresponds to mixing of CH_4 in the tunnel. It is measured after the mixing fan has created a homogeneous mixture after the injection procedure. As figure 4 shows, the value of RATIO is a series of plateaus corresponding to the time increments over which the CH_4 is well mixed. The value of RATIO increases with increasing CH_4 concentration for a fixed tunnel length or, equivalently, for increasing CH_4 pct•m. Also shown in figure 4 is the measured unnormalized ratio, which is a direct output from the ROM. The reduction in the initial peak value of the RATIO after the CH_4 is mixed is attributed to dilution of the CH_4 in the optical path during mixing. Because the CH_4 is injected into the optical path, higher readings were observed until the mixture became homogeneously mixed. This implies that once mixing is complete, CH_4 pct•m values obtained from the optical path will be reduced because the CH_4 was distributed over the entire volume of the tunnel, reducing the actual concentration in the optical path. The accumulated data from the 12 experiments are shown in figure 5. As expected, the RATIO increases as the CH_4 pct•m increases.

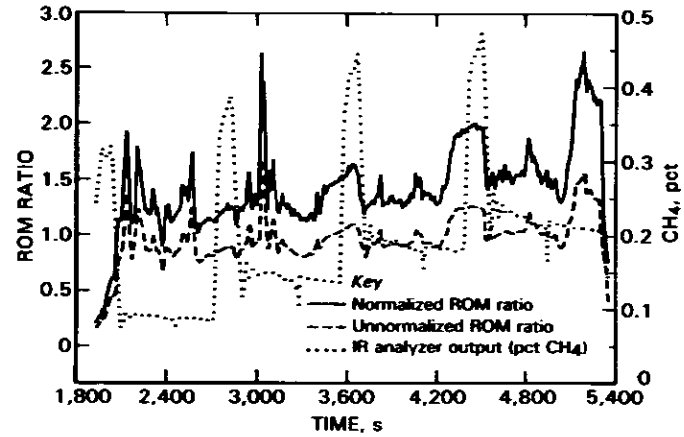

Figure 4.—Measured CH_4 concentration, ROM output signal RATIO, and calculated ROM RATIO.

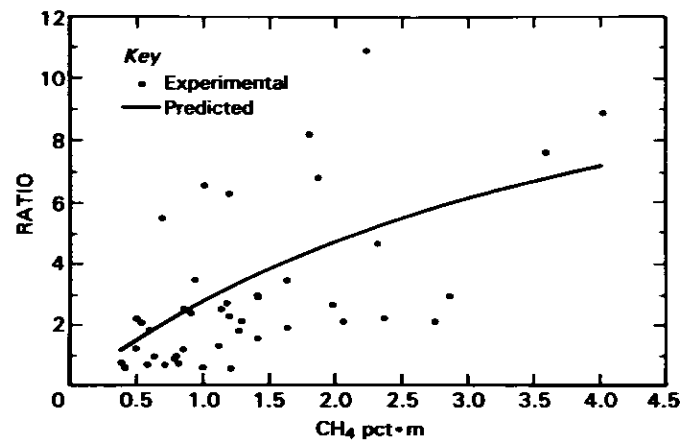

Figure 5.—RATIO versus pct CH_4•m for 12 experiments.

The ratio of the integrated signal to reference voltage can be defined in terms of the path length, ℓ, and the average CH_4 concentration, C, in the path using an absorption coefficient, α, (a specific characteristic of the detection system) for the CH_4:

$$\frac{V_S}{V_R} = e^{-2\alpha C\ell} \qquad (4)$$

The factor 2 accounts for the absorption of the infrared radiation over the distance, ℓ, from light source to target, which is traversed twice by the light. A regression analysis of the data in figure 5 yields an absorption coefficient of 0.158 (CH_4 pct•m)$^{-1}$. (If experiments I and L are excluded, due to higher values of the RATIO, or alternatively, lower values of V_S/V_R, the absorption coefficient determined by regression analysis is 0.082 (CH_4 pct•m)$^{-1}$ (indicating low response).) Figure 5 also shows the values of RATIO (solid line) calculated from equations 3 and 4 using α = 0.158 (CH_4 pct•m)$^{-1}$.

Several factors account for the scatter in the data in figure 5. These include (1) alignment of the optics in the ROM, (2) extraneous radiation that interferes with the infrared detector, i.e., the true zero of the instrument is changing with time due to heating within the field of view of the detector (gray body emissions), (3) electrical noise from circuit components, (4) inability to maintain adequate cooling of the infrared detector, and (5) variances in the alignment of the ROM within the calibration tunnel from test to test. The optical alignment has some dependence upon distance from detector to reflective surface and must be further investigated. The source of the extraneous radiation is the detector's case where the internal thermoelectric cooler deposits its heat. Efforts are being made to reduce the thermal energy storage in the case back plate and associated heat sink with the introduction of a conductive plate, with two external thermoelectric coolers attached, to the detector's heat sink. The use of a small fan on the heat sink of each thermoelectric cooler produced electromagnetic noise that interfered with the detector signal. Variances in the ROM alignment within the calibration tunnel are caused by variances in the angle of reflectance of the lamp light. This increases or decreases the returned light intensity. Decreased light intensity requires higher electronic gain in the amplifier stages to get an adequate signal for the processing electronics, and higher gains increase the noise interference to the instrument. Even if the thermal noise source is constant, increasing the detector gain also influences the rate at which the zero levels increase due to the gray body emissions.

CONCLUSION

A second-generation ROM was developed that is based on the replacement of the two-filter differential absorption technique with a single-filter gas correlation technique. Refinements were made to the amplifier and gating circuitry within the unit. Calibration tests in a specially constructed tunnel have shown that the ROM responds to increased CH_4 pct•m at distances as great as 11.6 m. The ROM is undergoing modifications to eliminate signal drift. These modifications are primarily in the design of a more efficient system for the dissipation of thermal energy generated by cooling of the infrared detector. It is anticipated that in the final version, the ROM will greatly improve miner safety by detecting hazardous CH_4 levels in deep cuts while the operator is under permanently supported roof.

ACKNOWLEDGMENT

The authors wish to acknowledge the helpful discussions held with C. D. Litton of the NIOSH Pittsburgh Research Center with regard to the operational principles and optical design of the ROM.

REFERENCES

CFR. Code of Federal regulations. Washington, DC: U.S. Government Printing Office, Office of the Federal Register.

Edwards JC, Li JS [1984]. Computer simulation of ventilation in multilevel mines. Proceedings of the Third International Mine Ventilation Congress. Harrogate, England, U.K.: Institution of Mining and Metallurgy/Institution of Mining Engineers, pp. 47-51.

Franks RA, Sapko MJ, Denes LJ, Ryan FM [1986]. Optical remote methanometer. Proceedings of the Eighth WVU Mining Electrotechnology Conference. Morgantown, WV: West Virginia University, pp. 114-118.

McPherson MJ [1992]. Subsurface ventilation and environmental engineering. New York, NY: Chapman and Hall, pp. 390-397.